EARTH SURFACE PROCESSES AND LANDFORMS
Earth Surf. Process. Landforms **36,** 439–448 (2011)

Published online 25 August 2010 in Wiley Online Library
(wileyonlinelibrary.com) DOI: 10.1002/esp.2057

Using beryllium-7 to monitor the relative proportions of interrill and rill erosion from loessal soil slopes in a single rainfall event

Gang Liu,[1,2] Ming Yi Yang,[2]* D.N. Warrington,[2] Pu Ling Liu[2] and Jun Liang Tian[2]

[1] Key Laboratory of Geological Hazards on Three Gorges Reservoir Area, Ministry of Education, China Three Gorges University, Yichang, Hubei, China

[2] State Key Laboratory of Soil Erosion and Dryland Farming on the Loess Plateau, Institute of Soil and Water Conservation, Chinese Academy of Science and Ministry of Water Resources, Northwest Sci-Tech University of Agriculture and Forestry, Yangling, Shaanxi, China

Received 8 September 2008; Revised 13 May 2010; Accepted 24 May 2010

*Correspondence to: Ming Yi Yang, State Key Laboratory of Soil Erosion and Dryland Farming on the Loess Plateau, Institute of Soil and Water Conservation, Chinese Academy of Science and Ministry of Water Resources, Northwest Sci-Tech University of Agriculture and Forestry, Yangling, Shaanxi, 712100, China.
E-mail: ymyzly@163.com

ESPL
Earth Surface Processes and Landforms

ABSTRACT: Quantifying the relative proportions of soil losses due to interrill and rill erosion processes during erosion events is an important factor in predicting total soil losses and sediment transport and deposition. Beryllium-7 (^{7}Be) can provide a convenient way to trace sediment movement over short timescales providing information that can potentially be applied to longer-term, larger-scale erosion processes. We used simulated rainstorms to generate soil erosion from two experimental plots (5 m × 4 m; 25° slope) containing a bare, hand-cultivated loessal soil, and measured ^{7}Be activities to identify the erosion processes contributing to eroded material movement and/or deposition in a flat area at the foot of the slope. Based on the mass balance of ^{7}Be detected in the eroded soil source and in the sediments, the proportions of material from interrill and rill erosion processes were estimated in the total soil losses, the deposited sediments in the flat area, and in the suspended sediments discharged from the plots. The proportion of interrill eroded material in the discharged sediment decreased over time as that of rill eroded material increased. The amount of deposited material was greatly affected by overland flow rates. The estimated amounts of rill eroded material calculated using ^{7}Be activities were in good agreement with those based on physical measurements of total plot rill volumes. Although time lags of 45 and 11 minutes existed between detection of sediment being removed by rill erosion, based on ^{7}Be activities, and observed rill initiation times, our results suggest that the use of ^{7}Be tracer has the potential to accurately quantify the processes of erosion from bare, loessal cultivated slopes and of deposition in flatter, downslope areas that occur in single rainfall events. Such measurements could be applied to estimate longer-term erosion occurring over larger areas possessing similar landforms. Copyright © 2010 John Wiley & Sons, Ltd.

KEYWORDS: deposition; runoff; hillslope geomorphology; sediments; simulated rainfall

Introduction

Soil erosion from hillslopes involves a complex sequence of processes that change during the course of an erosion event. Following transport by overland flow, eroded sediment from upper slopes may be partially deposited on lower gradient downslope areas, where flow rates have decreased, forming depositional areas (Theocharopoulos *et al*., 2003; Walling *et al*., 2003). During the erosion process, interrill, or sheet erosion, occurs initially and is later combined with rill erosion so that the deposited material may have been transported by either process. Rill erosion differs from interrill erosion in that the flow rates can be much higher and the carrying capacity of the flow is consequently greater. Consequently the magnitude of soil losses will depend on whether rill erosion is initiated or not, and for how long it occurs. The composition of the runoff sediment load can also be affected by the carrying capacity. For example, sediment originating from interrill processes may be either enriched (Warrington *et al*., 2009) or depleted (Young and Onstad, 1978) in clay compared with the parent soil material and with sediment removed by rill erosion. Whether enrichment or depletion occurs may be due to the soil types studied and/or the experimental conditions. However, knowing if clay enrichment or depletion is likely to occur due to the absence or presence of rill erosion can be important when estimating the risks of downstream pollution, since

pollutants are often preferentially bound to clay particles (Ghadiri and Rose, 1993). Likewise, understanding the processes involved in soil erosion is important in order to predict soil losses at various temporal and spatial scales and to evaluate the likely effectiveness of management methods intended to conserve soil.

Therefore, understanding the erosion–transport–deposition process is of primary importance to the development of physically based erosion prediction models (Merritt, 1984; Hancock *et al*., 2008). However, conventional erosion monitoring techniques do not provide enough information to distinguish between sediment removed by interrill erosion and that removed by rill erosion. Several frequently used, physically based erosion models such as WEPP (Water Erosion Prediction Project: Nearing *et al*., 1989; Laflen *et al*., 1991), LISEM (Limburg Soil Erosion Model: De Roo *et al*., 1994; De Roo, 1996) and EUROSEM (European Soil Erosion Model: Morgan *et al*., 1998) lack the capability to determine: (i) the time at which transport of sediments transitions from interrill to rill dominated processes; (ii) the relative contributions of these two processes during individual rainfall events. Furthermore, these models do not distinguish between the sediments removed by interrill and rill erosion processes, which may then be deposited at the base of the slopes. Use of beryllium-7 (^{7}Be) as a soil erosion tracer can provide more detailed information about soil erosion at specific locations.

^{7}Be is a short-lived radionuclide with a half-life of 53·4 days. It is produced naturally in the upper atmosphere by the spallation of nitrogen and oxygen atoms by cosmic rays. It then diffuses throughout the atmosphere until becoming attached to an atmospheric aerosol. Subsequent deposition on the land surface occurs as a result of both wet and dry fallout (Wallbrink and Murray, 1994; Rosner *et al*., 1996; Graham *et al*., 2003). In most environments, ^{7}Be fallout that reaches the soil surface will be rapidly and strongly fixed by clay particles (Wallbrink and Murray, 1996; Ródenas *et al*., 1997) where it is restricted to a shallow surface layer of about 20 mm, predominantly in the upper 10 mm (Wallbrink and Murray, 1993; Bai *et al*., 1996; Blake *et al*., 1999). Since interrill erosion generally occurs from the upper 10 mm of the soil, ^{7}Be should be ideally suited to trace soil losses from this layer.

A number of studies have used ^{7}Be as a tracer of soil erosion. Blake *et al*. (2002) evaluated ^{7}Be as a sediment tracer when used to investigate soil erosion and sediment mobilization from slopes; the transport, storage and remobilization of fine sediment in river channels; and overbank deposition on river floodplains. They concluded that the use of ^{7}Be had the potential to determine information pertinent to short-term and event-based sediment redistribution rates for use in catchment sediment budget investigations. Walling *et al*. (1999) analysed the spatial distribution characteristics of erosion and deposition in a cultivated field during a single rainfall event by using both ^{7}Be and cesium-137 (^{137}Cs). They similarly concluded that ^{7}Be was suitable for short- and medium-term studies of soil redistribution when used either by itself or in combination with ^{137}Cs.

Since differences exist between the depth distribution of ^{7}Be and that of other radionuclides such as ^{137}Cs and lead-210 (^{210}Pb) excess, the degree of erosion over time can be monitored when ^{7}Be is used in conjunction with them. Thus, Wallbrink and Murray (1993) identified a change from interrill erosion to minor rilling as the dominant erosion process by using ^{7}Be with ^{137}Cs and ^{210}Pb excess. Their study also confirmed the usefulness of ^{7}Be as a shallow surface soil source indicator. Whiting *et al*. (2001) developed a model to evaluate multiple mass balances for soil and radionuclides including ^{7}Be, ^{137}Cs and ^{210}Pb excess in order to quantify sheet and rill erosion mechanisms on slopes. In their study, rill erosion was determined to have produced 29 times more sediment than sheet erosion from a silty loam soil in a 6·03 ha agricultural field during a thunderstorm. Similarly, Yang *et al*. (2006a) quantifiably separated the sediment from sheet and rill erosion processes in small cultivated and uncultivated plots and described these changes as a function of runoff time. Although ^{7}Be has been useful in quantifying the process of soil erosion from slopes by overland flow, the effect of these processes on deposition at the foot of the slopes has been largely ignored. The usefulness of ^{7}Be as a tracer of short-term, shallow surface erosion over relatively small landscape areas should lend itself to such investigations. Furthermore, the results obtained from such studies have been found to be applicable to the understanding of longer-term erosion over larger landscape units in the absence of extreme erosion (O'Farrell *et al*., 2007).

The purpose of this research was to use ^{7}Be as a tracer to partition the sediment removed from bare, hand-cultivated, loessal soil plots by either interrill or rill erosion processes and to estimate their proportions in (1) the total soil loss, (2) the deposited material in a depositional area, (3) the suspended sediment carried beyond the depositional area and, where practical, the temporal variation in these processes. Furthermore, the measured quantities of eroded material were compared to those derived by calculations based on existing models. The accuracy of the calculated values, based on measured ^{7}Be activities within sediment samples, was assessed to determine whether the methodology could be used in the Loess Plateau region for this type of landform. Our findings were also intended to be of use to future studies related to the improvement or development of physically based erosion prediction models that would accurately quantify the processes of erosion using ^{7}Be as a tracer.

Methods and Materials

Experimental set-up

Two adjacent experimental plots, A and B, were constructed in the field to receive ^{7}Be fallout in Yangling County, Shaanxi Province, in the Loess Plateau region of China. Each plot (5 m long × 2 m wide; 25° slope) was separated by a plastic board so that one side (5 m × 0·5 m) would serve to characterize the distribution of ^{7}Be background activities, while the other side (5 m × 1·5 m) was used for the rainfall experiment (Figure 1). Two flat areas (0·3 m long × 1·5 m wide) with cement bases and bordered by sheet iron were constructed at the lower edge of the two plots to serve as depositional areas. Runoff and suspended sediments were funnelled by the sheet iron from the depositional area to an outlet for collection.

The two experimental plots were filled with soil taken from the upper 5 cm layer of a local, cultivated, silt loam soil. The soil comprised 12·3% clay, 58·85% silt (0·002–0·02 mm), and 28·85% sand (0·02–2 mm). The soil was gently packed, layer-by-layer, when filling the plot to give an average bulk density of 1·3 g cm^{-3}. After filling the plots, the surface layers, 0–20 cm, were hand tilled, large clods were broken up to less than about 5 cm in diameter, and the surface of the slopes were smoothed. The bulk density of the surface soil layer was determined to be 1·05 g cm^{-3} by sampling, which was similar to typical local tilled field conditions (Yang *et al*., 2006b). In order to reduce the influences of the plot borders, liquid bitumen was evenly daubed along the surfaces of the plastic boards inside the plots to fix the soil in contact with them. The two plots were left for six months (from November 2006 to April 2007), without human disturbance, in order to receive both wet and dry ^{7}Be fallout (Narazaki *et al*., 2003; Hirose

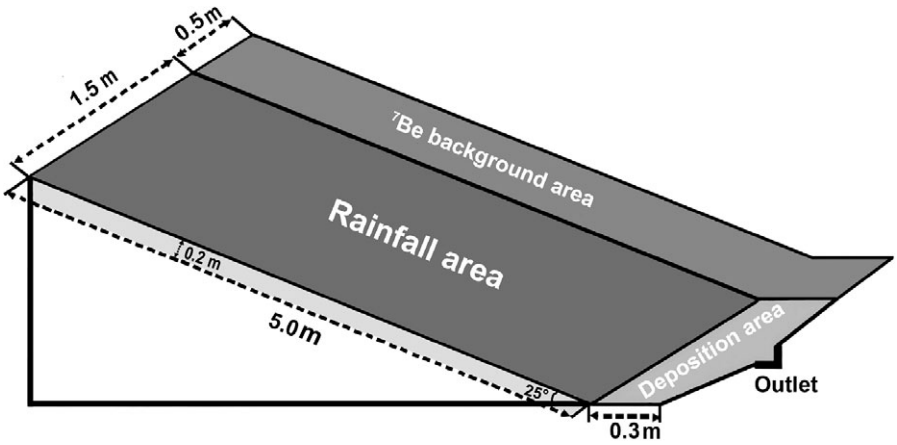

Figure 1. Schematic of the experimental plots.

et al., 2004). In this period there was little wind, and rainfall was predominantly of low intensity resulting in no observable erosion of the soil surface and a uniform distribution of ^{7}Be fallout over the slope.

Three nozzles positioned adjacent to the plots at a height of 4 m were used to spray tap water (electrical conductivity, 0·87 ds m^{-1}; sodium adsorption ratio, 1·94) sideways over the plots in order to simulate rainfall. Before adjustment of the nozzles, a piece of waterproof material was used to cover the plots. The nozzles were adjusted so that a vertically falling spray uniformly covered the entire soil surface. However, due to limitations of the experimental conditions (e.g. breeze and hydraulic pressure instability), the mean rainfall intensities, measured with rain gauges, differed between plots A and B and were 1·04 mm min^{-1} and 1·39 mm min^{-1}, respectively. Rainfall was applied separately to plots A and B for 155 and 69 minutes, equivalent to 161 and 96 mm of rain, respectively, in order to develop rills.

Sampling and laboratory analysis

Before applying the rainfall, an open-ended box (7 cm × 7 cm × 2 cm), slotted at 2 mm intervals, was used to collect five soil samples from the upper 2 cm soil depth of the background area of both plots. These samples were taken along the centre transect of the background area slopes at regularly spaced intervals, in order to characterize the mass depth (i.e. the sampling mass per unit area) distribution of ^{7}Be in the upper 10, 2 mm soil layers of each sample.

During the rainfall, a series of plastic containers was used to collect all of the runoff and sediment sequentially, in amounts of about 13 l each, at the outlet of each plot, noting the sampling times. For each container, the volume of water was measured and the sediment was air dried and weighed.

After the rainfall, 15 soil samples were collected from the upper 1·5 cm depth, from a grid (3 by 5 units) laid out over the soil surface. Each of the 15 samples was a composite sample of five subsamples taken within 10 cm of the centre of one grid unit (1 m × 0·5 m). In the flat depositional area, three whole depth sediment samples were removed in cores and then all of the remaining sediment was collected, air-dried, and weighed. The volume of every rill on the slope was determined using the method of Bruno *et al*. (2008) whereby the lengths of the rills and their cross-sectional areas were measured at multiple points.

All soil samples were ground to pass through a 1 mm sieve and placed in plastic cylinders, 7·7 cm long and 7·7 cm in diameter, thus having similar geometric dimensions as those used for the background ^{7}Be activity measurements.

Activities of ^{7}Be were measured using a low background, hyperpure, coaxial, germanium detector coupled to a multichannel digital analyser system (GMX-50220, EG&G ORTEC, Oak Ridge, TN). ^{7}Be was measured at 477·6 keV with a count time of more than 80,000 seconds. The detector was calibrated using standards of known activity and, from the calibration, was determined to have a precision of approximately ±6% at the 95% level of confidence. The measured ^{7}Be activities of the soil samples were converted to the activities at the time of sampling by using the appropriate decay constant.

The grain size distributions of the parent soil and of the sediments were measured using a laser granulometer (Mastersizer 2000, Malvern Instruments, Malvern, UK). All samples were pretreated with hydrogen peroxide to remove organic matter and chemically dispersed using sodium hexametaphosphate before analysis.

Calculations and data analysis

A relationship between ^{7}Be activities in the background area and mass depth was obtained by regression of the measured data to give an equation in the form:

$$C_{\mathrm{Be}} = ae^{-bH} \tag{1}$$

where C_{Be} is the ^{7}Be activity (in Bq kg^{-1}), H is the mass depth of soil (in kg m^{-2}), and a and b are constants determined by the regression.

The relative contributions of interrill and rill erosion were calculated based on a simple mass balance equation that relates the amount of soil associated with ^{7}Be activity that was removed from the plots to the amount of collected eroded material associated with ^{7}Be activity, as proposed by Yang *et al*. (2006a):

$$S \times \int_{0}^{H_{i,j}} ae^{bH} dH = \sum_{j=1}^{N} W_j \times C_{\mathrm{Be},j} \tag{2}$$

where S (in m^{2}) is the area of the experimental plot, the coefficients a and b describe the exponential mass depth (H; in kg m^{-2}) distribution of ^{7}Be in the surface soil layer (determined from Equation 1), and, for the jth time increment, W_j (in kilograms) is the weighed mass of collected sediment, $C_{\mathrm{Be},j}$ (Bq kg^{-1}) is the measured ^{7}Be activity of the collected sediment, and $H_{i,j}$ (in kg m^{-2}) is the mean mass depth of interrill erosion for the collected sediment determined from the measured ^{7}Be activity and Equation 1.

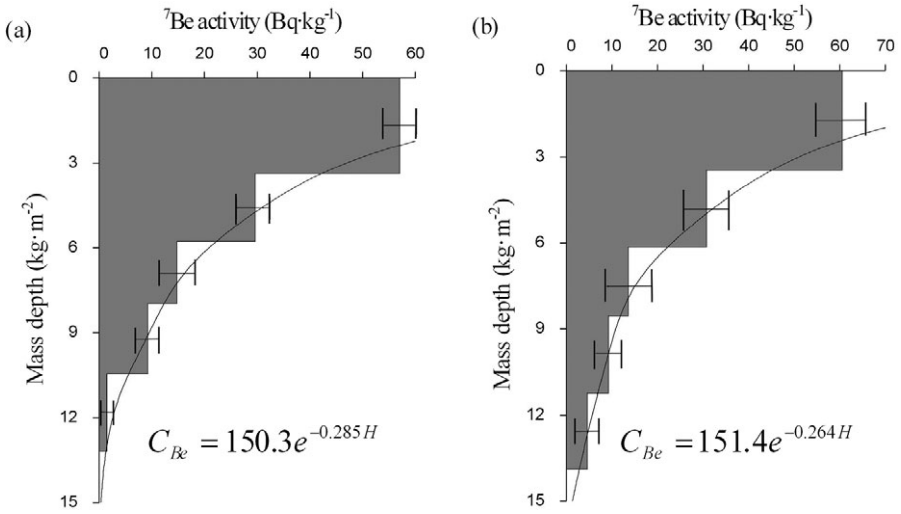

Figure 2. The vertical distribution of ^{7}Be activity in the cultivated loessal soil profile in the background area of (a) plot A and (b) plot B (shaded bars). Fitted exponential regression curves shown with derived equations where C_{Be} is ^{7}Be activity and H is the mass depth of soil. Error bars are ±1 standard deviation.

The mass balance equation assumes the various particle sizes in the eroded sediments are in the same proportions as the source material, i.e. the parent soil, and also that there is no redistribution among the soil particles during the erosion process. It is also reasonable to assume that interrill erosion occurs from the entire area of the plot, including the area occupied by rills. Furthermore, since rill erosion is commonly assumed to remove soil from below a soil depth of 1 cm (Poesen *et al*., 1998), and the soil at this depth would have much lower ^{7}Be activities than the uppermost layers of the surrounding soil being removed by interrill erosion, an approximation can be made that rill erosion does not contribute to the ^{7}Be activity detected in the sediments (Yang *et al*., 2006a). The mass of interrill erosion ($W_{i,j}$) in the collected sediment of the jth time increment is then given by:

$$W_{i,j} = (H_{i,j} - H_{i,j-1}) \times S \tag{3}$$

If rill erosion is occurring on the slope, the mass of collected sediment due to rill erosion in the jth time increment ($W_{r,j}$) is thus given by:

$$W_{r,j} = W_j - W_{i,j} \tag{4}$$

The total amount of soil removed by interrill erosion from the plot slope and deposited in the flat area at the base of the plot during the rainfall event was calculated from the following equations derived by Walling *et al*. (1999):

$$R_{Be} = h = h_0 \ln(A_{Be,ref} / A_{Be}) \tag{5}$$

which assumes that the interrill erosion is removed from successive depths in thin layers, where R_{Be} (in kg m^{-2}) is the soil erosion per unit area of the plot; h (in kg m^{-2}) is the mass depth of soil loss from the plot; h_0 (in kg m^{-2}) is the relaxation mass depth that is based on the shape of the ^{7}Be depth distribution for the uneroded points before the rainfall event and, for an exponential distribution with soil depth, has a value of 1/b where b is given by Equation 1; $A_{Be,ref}$ (in Bq m^{-2}) is the initial ^{7}Be reference inventory for the uppermost 1·5 cm soil layer, which was calculated by integrating Equation 1 for that specific soil layer; and A_{Be} (in Bq m^{-2}) is the ^{7}Be inventory determined to remain on the eroded slope from analysis of the samples taken following the rainfall, which is lower than the reference inventory, and reflects the depth of soil lost, h, at the sampling points. If the measured ^{7}Be inventory at the sampling point is larger than the local ^{7}Be reference inventory, deposition is assumed to have occurred.

Deposition of material from the plot slope in the depositional area, R'_{Be} (in kg m^{-2}), can be estimated from:

$$R'_{Be} = (A_{Be} - A_{Be,ref}) / C_{Be,d} \tag{6}$$

where $C_{Be,d}$ (in Bq kg^{-1}) is the ^{7}Be concentration in the deposited sediment. Decay of the ^{7}Be over the course of the experiment is assumed to be negligible.

Soil loss due to interrill erosion across the entire plot area (S) was determined from the mean depth of soil loss, $\bar{h}$, and the known soil bulk density (ρ) of the surface layer:

$$E_h = \bar{h} \cdot \rho \cdot S \tag{7}$$

where $\bar{h} = h/\rho$, where h was calculated from Equation 5, using the ^{7}Be activities determined for the samples taken from the eroded points on the slopes following the rainfall.

The amount of soil lost due to interrill erosion in the rill area (A_r) needs to be adjusted to consider the mass of soil (E_{ad}) removed from the rill area between the depths of $\bar{h}$ cm and 1 cm, since a common assumption is that the upper 1 cm of soil is always removed by interrill erosion during a typical rainfall event (Poesen *et al*., 1998; Zhang and Yasuhiro, 1998, Yang *et al*., 2006a):

$$E_{ad} = A_r (1 - \bar{h}) \rho \tag{8}$$

The total amount of soil lost from a plot due to interrill erosion (E_i) was thus determined from the sum of the interrill erosion occurring across the entire plot, including that occupied by rills, and the adjustment made for the rill area:

$$E_i = E_h + E_{ad} \tag{9}$$

Results and Discussion

Temporal changes of ^{7}Be activities in sediment

Figure 2 shows that the background levels of ^{7}Be activity in the surface layers of the background plots, A and B, decreased exponentially with an increase in mass depth. This result is consistent with the findings of other studies (e.g. Bai *et al*., 1996; Blake *et al*., 1999, etc.) and is related to the mechanism

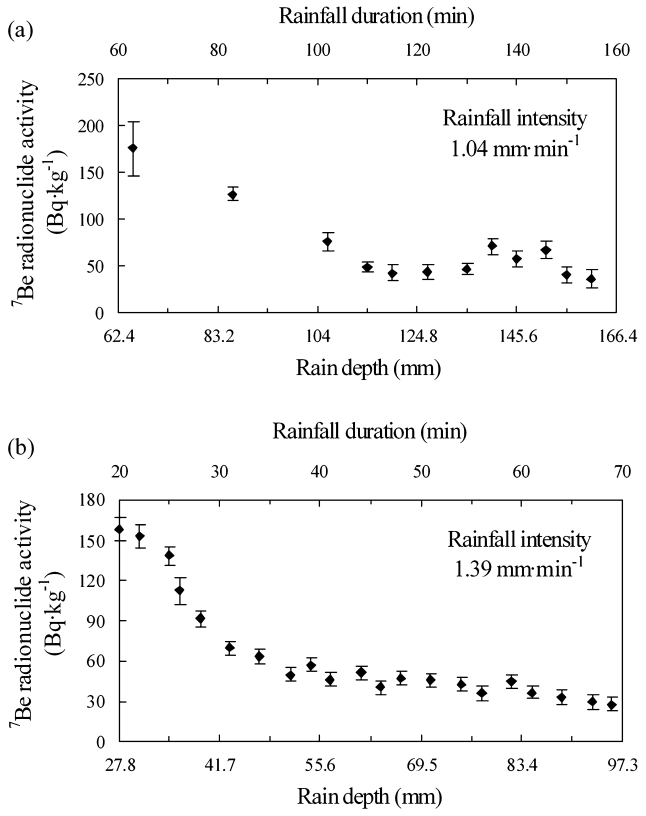

Figure 3. ^{7}Be activity of suspended sediment samples eroded from cultivated loessal soil plots during a simulated rainstorm for (a) plot A and (b) plot B. The error bars represent the precision of the γ spectrometry measurements at the 95% level of confidence.

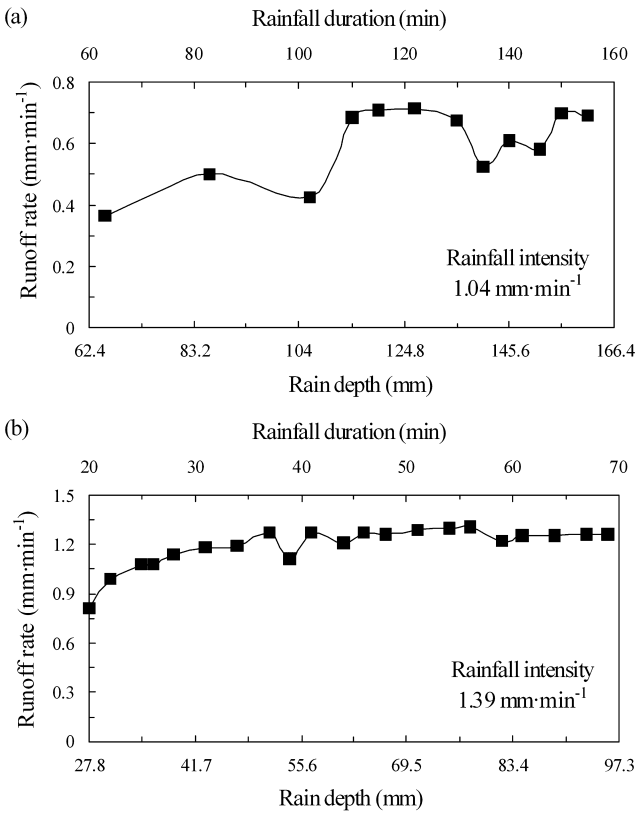

Figure 4. Runoff rate as a function of rainfall duration from cultivated loessal soil plots during a simulated rainstorm for (a) plot A and (b) plot B.

of aeolian dust deposition, and the mobility of ^{7}Be within the soil and its decay rate.

During our simulated rainfall events, runoff commenced 10 and 5 minutes after initiating rainfall on plots A and B, respectively. Soil was removed from the slope suspended as sediments in the runoff. Subsequently, some sediment was deposited in the flat area at the foot of the slope while the remainder was removed with the runoff water from the plot where it was collected. Figure 3 presents the ^{7}Be activities associated with the sediment collected from the outlets of the two plots during the course of the simulated rainfall events.

At the onset of interrill erosion, the collected sediments were associated with relatively large ^{7}Be activity values (Figure 3). The ^{7}Be activity values for the sediments collected later in the storm diminished with time to become relatively stable. Notably, the ^{7}Be activities of the initial sediment samples were much higher than that measured in the upper 2 mm layer of the soil (Figure 2). A possible explanation for this observation was that the ^{7}Be activity of the upper 2 mm layer was actually an average of the activities in the whole layer, which was stratified such that the greatest activity level would occur in the uppermost stratum. The regression curves for the relationship between ^{7}Be activity (C_{Be}) and mass depth (Equation 1) for the two background areas (Figure 2) were determined to be:

$$\text{Plot A: } C_{Be} = 150{\cdot}3e^{-0{\cdot}285H} \quad (n = 5, R^2 = 0{\cdot}996) \qquad (10)$$

$$\text{Plot B: } C_{Be} = 151{\cdot}4e^{-0{\cdot}264H} \quad (n = 5, R^2 = 0{\cdot}995) \qquad (11)$$

This indicated, by extrapolation, that the greatest levels of ^{7}Be activity could be 150·3 and 151·4 Bq kg^{-1} for plots A and B, respectively, for a mass depth of zero, which indicated that this explanation for the initially high ^{7}Be activities in the sediment was plausible. Furthermore, when the soil on the slope surface was eroded by interrill erosion, it could be assumed to have been removed layer-by-layer, although not necessarily at a uniform rate across the entire soil surface. Thus sediment collected in the first runoff samples likely originated almost entirely from the uppermost surface layer of soil on the slopes while that collected later in the storm probably came entirely from the lower soil depths (Walling *et al.*, 1999). Since these lower soil layers had lower ^{7}Be activities, which declined exponentially with mass depth (Figure 2), the ^{7}Be activities in the collected sediment thus similarly declined as the rainstorm progressed (Figure 3).

A second explanation for the large values of the ^{7}Be activities in the initial sediment samples was that enrichment of ^{7}Be may have occurred within them. Within the soil, ^{7}Be is more closely associated with the clay-sized fraction (Wallbrink and Murray, 1996). In the initial stage of a rainstorm, clay enrichment of sediments may occur (Monke *et al.*, 1977; Alberts *et al.*, 1983; Warrington *et al.*, 2009), which would in turn lead to relatively higher ^{7}Be activities. Clay enrichment usually occurs when the amount of overland flow is small and the carrying capacity of the runoff is low, and when more free clay is available for transport as a result of physicochemical dispersion by raindrops (Agassi *et al.*, 1981; Warrington *et al.*, 2009). Neither of these factors likely applied to our study. Use of tap water containing electrolytes to simulate rainwater likely reduced clay dispersion compared with situations where natural rainwater or deionized water was used (Agassi *et al.*, 1981). Furthermore, large values for ^{7}Be activity in the sediments persisted in samples collected when the runoff rate was already relatively large (Figure 4) suggesting that carrying capacity was a limiting factor at those times. A comparison of

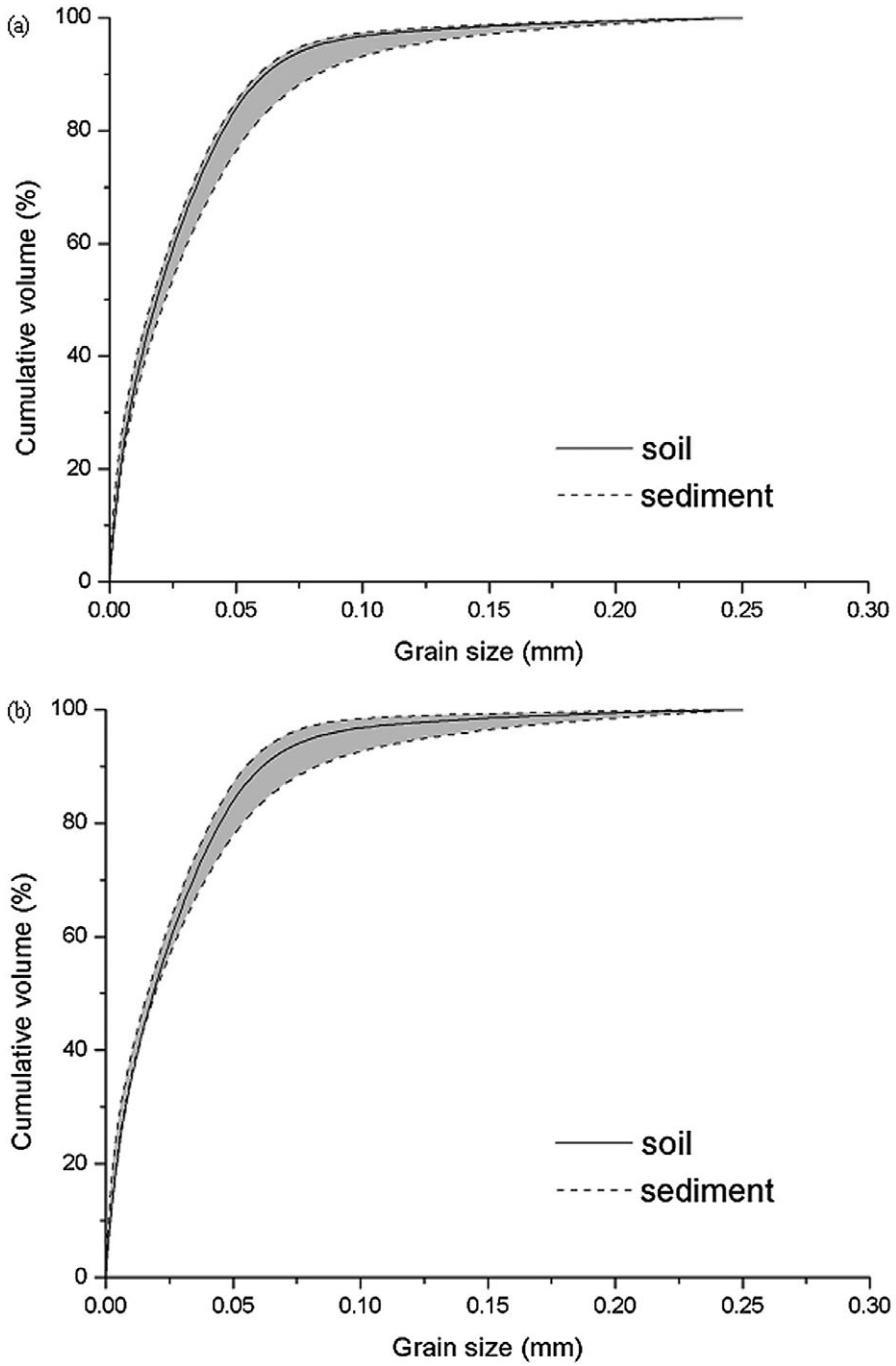

Figure 5. Particle size distribution (PSD) of the parent soil and the range of PSDs for the suspended sediments discharged from the cultivated loessal soil plots during simulated rainstorms for (a) plot A and (b) plot B.

the particle sizes of the sediments with those of the source soil also indicated that there was no significant difference between their particle size distributions, suggesting that little or no clay enrichment occurred (Figure 5). Figure 5 also shows that there was little change in the collected sediment particle size throughout the storms. Therefore, we concluded that clay enrichment was not a factor in producing the relatively high ^{7}Be activities in the initial sediment samples.

The ^{7}Be activities in the collected sediment from plots A and B had notably decreased after the first 102 and 36 minutes of the rainstorm to a comparatively steady level (Figure 3). The ^{7}Be activity of the sediment equalled that of the background samples in the upper 2 mm of soil at 100 and 30 minutes for A and B plots, respectively. As noted earlier, the initial decreases in ^{7}Be activity of the sediments may be ascribed to the fact that the source of the material comes from lower soil depths with correspondingly lower ^{7}Be activity levels as the interrill erosion process continues (Figures 2 and 3). The greater rate of decline in sediment ^{7}Be activity, most clearly seen in Figure 3 for plot B, suggested that the sediment now contained a greater proportion of material that originated from rill erosion processes. Sediment from rill erosion would come from deeper soil layers than those eroded by interrill processes and would, therefore, have appreciably lower ^{7}Be activity levels (Yang *et al*., 2006a).

During the experiment, the actual times when rills first appeared on the slope were 57 and 15 minutes after the rainstorm had commenced, for plots A and B, respectively, which was considerably earlier than the times when the rate of decline of ^{7}Be activities increased notably. The reason for this time lag between the observed initial development of rills and the detection of a sharp decrease in the ^{7}Be activity levels in the sediment was likely due to the time that it takes for the amount of sediments coming from the rills to become proportionally large enough, compared with those from the interrill areas, to affect the ^{7}Be activity levels of the entire sediment load. This time would, in turn, be related to the rate of development of the rill system and the increased size of the rill area.

Table I. Changes over time in the ^{7}Be activity of sediments ($C_{Be,j}$) eroded during simulated rainstorms on cultivated plots for time intervals (j), and the measured total soil losses (W_j) and associated estimates of interrill ($W_{i,j}$; W_i) and rill ($W_{r,j}$; W_r) erosion with their relative contributing ratios

Plot	j	Rainfall time (min)	$C_{Be,j}$ (Bq kg^{-1})	W_j(g)	$W_{i,j}$(g)	$W_{r,j}$(g)	$W_{i,j}/W_j$ (%)	$W_{r,j}/W_j$ (%)
A	1	0–63	176·03±28·39	196	196	0	100·0	0·0
	2	63–83	127·17±7·08	258	221	37	85·7	14·3
	3	83–102	75·92±9·77	222	114	108	51·5	48·5
	4	102–110	49·08±5·30	370	124	246	33·4	66·6
	5	110–115	42·58±8·38	253	74	179	29·1	70·9
	6	115–122	43·77±7·41	234	70	164	30·0	70·0
	7	122–130	46·75±6·75	312	100	212	32·2	67·8
	8	130–135	71·24±8·66	197	97	100	49·2	50·8
	9	135–140	57·09±8·48	230	91	139	39·6	60·4
	10	140–146	67·50±9·36	192	90	102	47·0	53·0
	11	146–150	40·27±8·90	254	71	183	28·1	71·9
	12	150–155	36·68±10·61	170	44	126	25·6	74·4
		Total (kg)		W = 2·9	W_i = 1·3	W_r = 1·6	W_i/W = 44·8	W_r/W = 55·2
B	1	0–20	158·45±8·76	273	273	0	100·0	0·0
	2	20–22	152·84±9·10	260	260	0	100·0	0·0
	3	22–25	138·01±7·51	331	309	22	93·5	6·5
	4	25–26	112·20±10·23	230	176	54	76·7	23·3
	5	26–28	91·35±6·25	328	206	122	62·8	37·2
	6	28–31	69·36±4·87	633	305	328	48·1	51·9
	7	31–34	63·44±5·15	686	305	381	44·5	55·5
	8	34–37	49·25±4·92	767	268	499	34·9	65·1
	9	37–39	56·88±4·88	889	362	527	40·8	59·2
	10	39–41	46·23±5·22	628	210	418	33·5	66·5
	11	41–44	51·18±4·85	590	220	370	37·3	62·7
	12	44–46	40·02±4·74	672	198	474	29·4	70·6
	13	46–48	47·33±4·82	738	259	479	35·0	65·0
	14	48–51	45·60±5·08	644	219	425	34·0	66·0
	15	51–54	42·49±5·64	567	181	386	32·0	68·0
	16	54–56	36·13±5·20	647	177	470	27·3	72·7
	17	56–59	44·55±4·86	660	224	436	34·0	66·0
	18	59–61	36·17±4·82	837	233	604	27·8	72·2
	19	61–64	32·33±5·42	915	229	686	25·0	75·0
	20	64–67	29·72±5·44	941	218	723	23·2	76·8
	21	67–69	27·69±5·22	511	111	400	21·7	78·3
		Total (kg)		W = 12·7	W_i = 4·9	W_r = 7·8	W_i/W = 38·6	W_r/W = 61·4

At the observed time of the initiation of the rill system, very little eroded material came from the rills. Furthermore, the approximation made for Equations 3 and 4, namely that the ^{7}Be activity levels of sediment removed by rill erosion processes did not affect the overall ^{7}Be activity level of the sediment samples, may not be completely accurate and may have contributed to the observed time lag.

The possibility that the models used to distinguish between eroded material from the rill and interrill erosion processes might be inaccurate is a cause for concern. Future work could test the models by comparing their output with calculations based on rill volumes measured continuously throughout a storm using three-dimensional digital imagery.

Fluctuations in ^{7}Be activities that deviated from the general trend were probably caused by the development of the rill system, which was not a uniform process. This non-uniform process would also result in fluctuations in the runoff rate (Figure 4), which in turn affects the amount of sediment carried from the slope (Nearing, 1988; Lei *et al*., 1998).

The relative contributions of interrill and rill erosion

We assumed that the particle size distribution of the collected eroded sediments was not significantly different from the parent material when calculating the relative contributions of interill and rill erosion. Figure 5 compares the particle size distribution of the parent material, determined from the composite of the background samples, to that of all of the collected sediment samples, shown as a range of distributions denoted by the shaded area. Figure 5 indicates that the assumption was valid. Furthermore, it can be reasonably assumed that there was little redistribution of the particles during the erosion and deposition processes. All of the sediment carried from the slopes by the runoff was either deposited in the initially empty, flat, concreted area or was carried out of the plot to the collection containers. Hence, we used Equations 2, 3, 4, 10 and 11 to calculate the masses of eroded material removed from plots A and B by interrill and rill erosion processes and presented these values in Table I.

From Table I it can be seen that, as the rainstorm progressed, the mass of eroded material from rill erosion relative to that from interrill erosion generally increased. Thus, it contributed nothing to the erosion process initially but was responsible for the removal of more than half of the eroded material after 102 and 26 minutes of rainfall, equivalent to 61% and 27% of the total rainfall periods, for plots A and B, respectively. The contribution ratio of interrill to rill erosion masses fluctuated during the rainfall event and, as noted earlier, was likely due to erratic rill formation processes that also influenced runoff rates. Over the entire rainstorm, the percentages of sediment resulting from rill erosion were 55·2% from plot A and 61·4% from plot B.

Table II. Calculation of interrill erosion from the two plots

Parameter name	Parameter	Plot A	Plot B	Derivation	Equations
Relaxation mass depth	h_0 (kg m^{-2})	3·5	3·8	Calculated	5, 10, 11
Initial ^{7}Be reference inventory for the top 1·5 cm soil layer	$A_{Be,ref}$ (Bq m^{-2})	392·6	438·2	Measured	
Mass depth of soil loss	h (kg m^{-2})	0·27	0·30	Calculated	5
Soil loss due to interrill erosion	E_h (kg)	2·0	2·3	Calculated	7
Rill area	A_r (m^2)	0·17	0·32	Measured	
Extra masses of soil removed from the $\bar{h}$ to 1 cm soil depth	E_{ad} (kg)	1·7	3·3	*Calculated*	8
Total amount soil loss due to interrill erosion	E_i (kg)	3·7	5·6	Calculated	9

Table III. Measured and predicted parameters of eroded sediment mass from the two bare, cultivated, loessal soil plots (A and B)

	Sediment mass (kg)		Contribution (%)		Relative errors (%)			
Parameters	Plot A	Plot B	Plot A	Plot B	Plot A	Plot B	Derivation	Equations or method
W	2·9	12·7					Measured	Weighed
W_i	1·3	4·9	44·8	38·6			Calculated	2, 3, 10, 11
W_r	1·6	7·8	55·2	61·4			Calculated	4
D	6·1	3·7					Measured	Weighed
D	6·7	4·1			9·8	10·8	Calculated	6
D_i	2·4	0·7	*39·3*	*18·9*			*Calculated*	$E_i - W_i$
D_r	3·7	3·0	60·7	81·1			Calculated	$D - D_i$
E_i	3·7	5·6	45·1	37·3			Calculated	9
E_r	4·5	9·4	54·9	62·7			Measured	Rill volume
E_r	5·3	10·8			17·8	14·9	Calculated	$D_r + W_r$
E	9·0	16·4					Calculated	$D + W$

Where E is the mass of soil loss from the slope, W is the sediment removed from the plot, and D is the mass of sediment deposited in the depositional area of the plots; subscripts i and r designate material from interrill and rill erosion, respectively. Parameters were either measured directly or calculated using either the ^{7}Be tracer data or physical measurements of rill volume.

An increase in the contribution of rill erosion processes to the eroded sediment over the course of the rainstorm was expected since rill system development would produce higher runoff flow rates with higher carrying capacities within the rill channels.

Interrill erosion contribution to total sediment deposition

Distribution of ^{7}Be due to natural fallout over the area of the slope was found to be approximately uniform before the rainfall (Figure 2). The vertical distribution of ^{7}Be in the background reference plots conformed to the exponential distribution assumed for the equations derived by Walling *et al*. (1999) (Figure 2). From the measured vertical distribution of the ^{7}Be in the soil in these areas, we calculated the relaxation depth, h_0, and the initial ^{7}Be reference inventory, $A_{Be,ref}$, on the slopes exposed to rainfall (Table II). The value of $A_{Be,ref}$ on the flat area of the plots was zero because there was no soil in this area before the rainfall.

The total amount of soil lost from a plot due to interrill erosion (E_i) was determined from the sum of the interrill erosion occurring across the entire plot, including that occupied by rills, with an adjustment made for the rill area. Table II presents the results of the calculations. The lower amounts of interrill eroded material from plot A, when compared with those from plot B, were likely due to the lower overland flow rates. These were in turn due to the lower rainfall intensity applied to plot A, which also resulted in a reduction in the degree and rate of seal formation (see earlier). Consequently, 1·5 times more interrill erosion occurred from plot B than from plot A. Since interrill erosion removes the upper layers of the soil, it carries with it potential pollutants associated with the soil surface such as pesticides, herbicides and the products of atmospheric deposition. Knowing the degree of interrill erosion could be used to assess the fate and impact of these substances in the environment following translocation.

The total amounts of deposition (D) in the flat area of plots A and B were calculated from the ^{7}Be activities of the deposited material using Equation 6 and were found to be 6·7 kg and 4·1 kg, respectively. When compared to the measured mass found in the flat area, the relative error between calculated and measured amounts of deposition were about 10% for both plots (Table III). This indicates that the Walling model was reasonably accurate in predicting deposition rates in our experiment. Furthermore, some of the error could possibly be attributable to the heterogeneity of the distribution of the deposited material and the errors associated with obtaining a representative sample of this material. Future studies could investigate the spatial distribution, both vertically and horizontally, of deposited material over small scales using ^{7}Be as a tracer.

The relative contributions of interrill and rill erosion to the soil loss, deposited material and suspended sediment

Based on the mass balance between eroded soil and sediment, the experimental data and the equations described earlier, it is possible to determine the contributions of interrill and rill erosion to total soil loss, the deposited material and the suspended sediments (Table III).

The amount of rill erosion (E_r) from the slopes of plots A and B estimated using Walling's equations had a relative error of

17·8% and 14·9% compared to calculations based on the measured rill volume below a rill depth of 1 cm (Table III). The latter method is laborious and time consuming and is inaccurate due to simplifications made about rill morphology. The use of ^{7}Be could be a more convenient way to get a practical estimate of rill erosion. As noted earlier, further testing of the model is required.

Table III presents the calculated relative contributions of interrill erosion to the soil lost from the plot slope and to the sediment that was either deposited in the flat area or removed from the plot. Interrill erosion was a greater relative contributor of eroded material in both the deposited and suspended sediments for plot A than for plot B. Thus, although the rainfall time for plot A was greater than for plot B, the relative contributions of rill erosion to the total soil loss, deposited material and suspended sediments from the slope of plot A were smaller than that from the slope of plot B. This can be ascribed to the relative lack of rill development in plot A due to the lower rainfall intensity. The consequent reduction in the rate of surface sealing resulted in smaller amounts of runoff with lower flow rates, shear forces and carrying capacity than from plot B (Figure 4). With higher flow rates, greater amounts of soil were lost from the slope of plot B than from that of plot A. Furthermore, the ratio of suspended sediment to deposited material was 3·43:1 for plot B compared to only 0·48:1 for plot A, since more material was carried out of plot B (Table III).

Applications

The use of ^{7}Be appears to be a useful and reasonably accurate tool that distinguished between interrill- and rill-derived eroded material in the total soil losses from our slopes, and within the sediment that was either deposited or carried out of the plots. This suggests that the method can be applied to landscape units with similar sizes and features (i.e. loessal slopes that adjoin flatter areas such as artificial or natural benches) to assess the impact of depositional processes on soil losses from natural slopes. Data derived from such small-scale units could be used in combination with the input and output data of surrounding units to build a process driven model to predict soil erosion at the landscape scale. Such models can be tested against data using ^{7}Be activities measured at the landscape scale (Wallbrink and Murray, 1996; Walling *et al*., 1999). Assuming a landscape is not subjected to extreme, atypical erosion events, the data collected for erosion events of short duration could be used to assess long-term erosion processes in the landscape (O'Farrell, 2007). However, interactions and feedbacks between erosion processes at large scales may complicate and limit the construction of such models.

Since rill erosion causes relatively greater soil loss than interrill erosion, this technique could be used to determine when rill erosion becomes a significant contributor to overall soil losses. Factors such as slope length, soil infiltrability dynamics, typical rainfall intensities and surface cover would need to be considered. Given information about when rills will develop, land managers could use this information to devise appropriate counter-measures that may include the creation of artificial benches, terraces, vegetative barriers, and/or the use of mulch and soil amendments. Preventing rill formation and limiting soil erosion to interrill processes where possible is also desirable since rills formed in one rainstorm persist throughout a rainy season or for years, providing ready made channels for concentrated runoff flow. In the case of the Loess Plateau, severe soil erosion leads to the formation of extensive rill systems that eventually form gullies (Yang *et al*., 2006b). On a practical level, use of ^{7}Be may not be viable in all situations. However, in combination with automatic sampling systems, the method lends itself to a convenient way to assess rill initiation without the need for human presence.

As noted earlier, deposition of material over short spatial scales such as those used in our study may be of interest in the study of spatial variability of soil properties. Use of ^{7}Be could enhance such studies by identifying the erosion process by which deposited material was delivered to the depositional area and how each process contributes to soil spatial variability. It may also resolve the issue of the extent of the error ascribed earlier to spatial variability that was observed between measured and predicted deposition.

Finally, soil type may have an effect on primary particle size distributions in the sediment, especially during the initial phases of a rain storm, as reported by Warrington *et al*. (2009) who also noted that the rate of soil wetting may be a factor. Since one of the assumptions made in the calculations is that primary particle sizes are similar for the source and sediment material, this is a factor that must be considered when using this methodology.

Conclusions

We used the distribution of natural ^{7}Be fallout in the surface soil of two plots filled with a bare, cultivated, loessal soil to quantitatively estimate proportions of sediments that were associated with either interrill or rill erosion. We analysed ^{7}Be activities in the collected eroded material that was either deposited within a depositional area or removed in runoff water from the plots. During simulated rainstorms, the estimated proportion of interrill erosion in the sediment gradually declined as that of rill erosion increased. A time lag was observed between observed rill development commencing and evidence of sediment attributed to rill erosion being detected in sediment samples. This was attributed to the time that it takes to develop a rill system that produces an amount of sediment that was proportionally large enough, compared with those from the interrill areas, to affect the ^{7}Be activity levels of the entire sediment load.

The calculated masses of soil lost through rill erosion and of deposited sediments based on sediment mass balance equations and ^{7}Be activities were similar to values obtained by direct measurement. Thus, proportions of material related to interrill and rill erosion processes could be accurately estimated with respect to the soil losses from the plot slopes, deposition in the flat areas of the plot, and the sediments carried from the plot suspended in runoff water.

We concluded that, in general, using ^{7}Be to study the processes of interrill and rill erosion from a short slope during rainfall events can be accurate and advantageous. Integrating the use of the ^{7}Be tracer, monitoring sediment, simulating rainfall and *in situ* measurements is an effective methodology for studying erosion processes in relation to landscape features. More work is needed in order to apply the approach described here to the investigation of the temporal and spatial processes of deposition, especially over scales similar to those we used. An understanding of the processes involved in soil erosion is important, not only in deriving process-driven mathematical models that more accurately predict soil losses at various temporal and spatial scales, but also in evaluating the likely effectiveness of management methods intended to conserve soil.

Acknowledgements—The financial support for the work described in this paper was provided by the National Basic Research Program of

China (973 Program) (No.2007CB407201), the Program for New Century Excellent Talents in University, the Open Research Fund Program of the State Key Laboratory of Soil Erosion and Dryland Farming on the Loess Plateau (Grant No. 10501-266), and the Scientific Research Foundation of China Three Gorges University (Grant No. KJ2009B033 and KJ2009A002). The authors are grateful to the National Engineering Research Centre for Water Saving Irrigation for providing the experimental facilities for the rainstorms. We wish to express our appreciation to Zhan MH and Li YQ for their help in data collection.

References

Agassi M, Shainberg I, Morin J. 1981. Effect of electrolyte concentration and soil sodicity on infiltration-rate and crust formation. *Soil Science Society of America Journal* **45**: 848–851.

Alberts EE, Wendt RC, Piest RF. 1983. Physical and chemical properties of eroded soil aggregates. *Transactions of the American Society of Agricultural Engineers* **26**: 465–471.

Bai ZG, Wan GJ, Wang CS, Wan X, Huang RG, Santschi PH, Baskaran M. 1996. ^{7}Be: a geochemical tracer for seasonal erosion of surface soil in watershed of Lake Hongfeng, Guizhou, China. *Pedosphere* **6**: 23–28.

Blake WH, Walling DE, He Q. 1999. Fallout beryllium-7 as a tracer in soil erosion investigations. *Applied Radiation and Isotopes* **51**: 599–605.

Blake WH, Walling DE, He Q. 2002. Using cosmogenic beryllium-7 as a tracer in sediment budget investigations. *Geografiska Annaler: Series A, Physical Geography* **84**: 89–102.

Bruno C, Stefano CD, Ferro V. 2008. Field investigation on rilling in the experimental Sparacia area, South Italy. *Earth Surface Processes and Landforms* **33**: 263–279.

De Roo APJ. 1996. The LISEM project: an introduction. *Hydrological Processes* **10**: 1021–1025.

De Roo APJ, Wesseling CG, Cremers NHDT, Offermans RJE, Ritsema CJ, Van Oostindie K. 1994. LISEM: a new physically-based hydrological and soil erosion model in a GIS-environment, theory and implementation. In *Variability in Stream Erosion and Sediment Transport*, Proceedings of the Canberra Symposium, IAHS Publication 224. International Association of Hydrological Sciences (IAHS): Wallingford; 439–448.

Ghadiri H, Rose CW. 1993. Water erosion processes and the enrichment of sorbed pesticides. Part 1. Enrichment mechanisms and the degradation of applied pesticides. *Journal of Environmental Management* **37**: 23–35.

Graham I, Ditchburn R, Barry B. 2003. Atmospheric deposition of ^{7}Be and ^{10}Be in New Zealand rain (1996–98). *Geochimica et Cosmochimica Acta* **67**: 361–373.

Hancock GR, Crawter D, Fityus SG, Chandler J, Wells T. 2008. The measurement and modelling of rill erosion at angle of repose slopes in mine spoil. *Earth Surface Processes and Landforms* **33**: 1006–1020.

Hirose K, Honda T, Yagishita S, Igarashi Y, Aoyama M. 2004. Deposition behaviors of ^{210}Pb, ^{7}Be and thorium isotopes observed in Tsukuba and Nagasaki, Japan. *Atmospheric Environment* **38**: 6601–6608.

Laflen JM, Lane LJ, Foster GR. 1991. The Water Erosion Prediction Project – a new generation of erosion prediction technology. *Journal of Soil and Water Conservation* **46**: 34–38.

Lei T, Nearing MA, Haghighi K, Bralts VF. 1998. Rill erosion and morphological evolution: a simulation model. *Water Resources Research* **34**: 3157–3168.

Merritt E. 1984. The identification of four stages during micro-rill development. *Earth Surface Processes and Landforms* **9**: 493–496.

Monke EJ, Marelli HJ, Meyer LD, Dejong JF. 1977. Runoff, erosion, and nutrient movement from interrill areas. *Transactions of the American Society of Agricultural Engineers* **20**: 58–61.

Morgan RPC, Quinton JN, Smith RE, Govers G, Poesen JWA, Auerswald K, Chisci G, Torri D, Styczen ME. 1998. The European Soil Erosion Model (EUROSEM): a dynamic approach for predicting sediment transport from fields and small catchments. *Earth Surface Processes and Landforms* **23**: 527–544.

Narazaki Y, Fujitaka K, Igarashi S, Ishikawa Y, Fujinami N. 2003. Seasonal variation of ^{7}Be deposition in Japan. *Journal of Radioanalytical and Nuclear Chemistry* **256**: 489–496.

Nearing MA, West LT, Brown LC. 1988. A consolidation model for estimating changes in rill erodibility. *Transactions of the American Society of Agricultural Engineers* **31**: 696–700.

Nearing MA, Foster GR, Lane LJ, Finkner SC. 1989. A process-based soil erosion model for USDA-Water Erosion Prediction Project technology. *Transactions of the American Society of Agricultural Engineers* **32**: 1587–1593.

O'Farrell CR, Heimsath AM, Kaste JM. 2007. Quantifying hillslope erosion rates and processes for a coastal California landscape over varying timescales. *Earth Surface Processes and Landforms* **32**: 544–560.

Poesen JWA, Vandaele K, van Wesemael B. 1998. Gully erosion: importance and model implications. In *Modelling soil erosion by water*, Boardman J, Favis-Mortlock D (eds), NATO ASI Series, Series I: Global Environmental Change 55. Springer: Berlin; 285–312.

Rosner G, Hötzl H, Winkler R. 1996. Continuous wet-only and dry-only deposition measurements of ^{137}Cs and ^{7}Be: an indicator of their origin. *Applied Radiation and Isotopes* **47**: 1135–1139.

Ródenas C, Gómez J, Quindós LS, Fernández PL. 1997. ^{7}Be concentrations in air, rain water and soil in Cantabria (Spain). *Applied Radiation and Isotopes* **48**: 545–548.

Theocharopoulos SP, Florou H, Walling DE, Kalantzakos H, Christou M, Tountas P, Nikolaou T. 2003. Soil erosion and deposition rates in a cultivated catchment area in central Greece, estimated using the ^{137}Cs technique. *Soil & Tillage Research* **69**: 153–162.

Wallbrink PJ, Murray AS. 1993. Use of fallout radionuclides as indicators of erosion processes. *Hydrological Processes* **7**: 297–304.

Wallbrink PJ, Murray AS. 1994. Fallout of ^{7}Be in south eastern Australia. *Journal of Environmental Radioactivity* **25**: 213–228.

Wallbrink PJ, Murray AS. 1996. Distribution and variability of ^{7}Be in soils under different surface cover conditions and its potential for describing soil redistribution processes. *Water Resources Research* **32**: 467–476.

Walling DE, He Q, Blake WH. 1999. Use of ^{7}Be and ^{137}Cs measurement to document short and medium-term rates of water-induced soil erosion on agricultural land. *Water Resources Research* **35**: 3865–3874.

Walling DE, Collins AL, Sichingabula HM. 2003. Using unsupported lead-210 measurements to investigate soil erosion and sediment delivery in a small Zambian catchment. *Geomorphology* **52**: 193–213.

Warrington DN, Mamedov AI, Bhardwaj AK, Levy GJ. 2009. Primary particle size distribution of eroded material affected by degree of aggregate slaking and seal development. *European Journal of Soil Science* **60**: 84–93.

Whiting PJ, Bonniwell EC, Matisoff G. 2001. Depth and areal extent of sheet and rill erosion based on radionuclides in soils and suspended sediment. *Geology* **29**: 1131–1134.

Yang MY, Walling DE, Tian JL, Liu PL. 2006a. Partitioning the contributions of sheet and rill erosion using beryllium-7 and cesium-137. *Soil Science Society of America Journal* **70**: 1579–1590.

Yang MY, Tian JL, Liu PL. 2006b. Investigating the spatial distribution of soil erosion and deposition in a small catchment on the Loess Plateau of China, using ^{137}Cs. *Soil & Tillage Research* **87**: 186–193.

Young RA, Onstad CA. 1978. Characterization of rill and interrill eroded soil. *Transactions of the American Society of Agricultural Engineers* **21**: 1126–1130.

Zhang KL, Yasuhiro A. 1998. Critical hydraulic condition of rill erosion on sloping surface. *Journal of Soil Erosion and Soil and Water Conservation* **4**: 41–46 (in Chinese, with English abstract).

